2005 SCEC ANNUAL REPORT

Project Title: Developing and Validating a Method for Prediction of Broadband Time Histories
Principal Investigators: Pengcheng Liu and Ralph Archuleta
Institution: Institute for Crustal Studies, University of California, Santa Barbara

Introduction

With increasing usage of nonlinear analysis techniques in the seismic design of structures, synthesizing time histories of ground motion becomes more important for the complete determination of structural response and damage estimation from future large earthquakes. While we cannot know the exact time of the next damaging earthquake, geologists, seismologists and geodesists have delineated faults that are capable of producing large magnitude earthquakes in urban areas. For example recent work by Shaw and others (2002) has spotlighted the Puente Hills thrust fault system that underlies the Los Angeles metropolitan area. This system is capable of producing earthquakes from M_W 6.5 to 7.2 with serious economic and humankind consequences (Field *et al.*, 2005).

Within a few fault lengths and at frequencies of engineering interest (0.1 to 20 Hz), ground motion estimates strongly depend on fault geometry, detailed rupture processes, wave propagation paths, and local site conditions. All of these characteristics are complicated, and an accurate description of most of them is not readily available. As a consequence we are forced to make many assumptions when constructing source models and generating Green's functions in order to estimate ground motions.

A credible model of the complex source process is essential for the prediction of ground motion. Although efforts have been made to implement the dynamic modeling of extended source models to predict ground motions (Guatteri, *et al.*, 2003, Hartzell, *et al.*, 2004), high-frequency dynamic fault models are still quite difficult and computationally expensive. Although the computational limits can be overcome to some degree, these models will be restricted to low frequencies (less than 2-3Hz). Kinematic modeling remains as one of the best means to incorporate many aspects of physical models of the earthquake process while still being able to compute broadband strong ground motion.

Besides the complications due to the source, complex Earth models significantly influence the amplitude, frequency content, and duration of ground motions. Any accurate ground motion estimate must include Green's functions that encompass, or try to encompass, the complexity of the velocity structure. In addition, the nonlinear site effects is another important issue should be addressed in ground motion prediction, because strong ground motions, especially the high-frequency ground motions, can induce non-linear soil response near the surface.

We present a new method for computing broadband strong ground motions. We have developed a technique for kinematic modeling of an extended earthquake source that is based on distribution functions for the slip amplitude, duration of slip (risetime) and rupture time. The complexity of the source process is represented by spatial distributions of randomized source parameters, but the integrated characteristics of these parameters will be constrained by the total moment (magnitude), radiated energy and the high-frequency decay of the spectral amplitudes in the source spectrum.

Having the kinematic source model, we use a three-dimensional Earth velocity structure to calculate synthetic ground motions for frequencies up to one to two Hertz. We also compute ground motions with the frequency up to 15-20 Hz using a 1D model. The 1D synthetics are first

deconvolved to the bedrock level using the available geotechnical information. This bedrock time history is propagated to the surface using a 1D nonlinear wave propagation code (e.g., Bonilla *et al.*, 1998; Hartzell *et al.*, 2004). The 3D ground motions (low-frequency) and high-frequency components of 1D ground motions (with consideration of nonlinear effects) are stitched together to form the broadband time histories of ground motions. The data set from the 1994 Northridge earthquake is used to validate this prediction method.

Method for Prediction of Ground Motions

We have developed a new method and a computer code to simulate stochastically the kinematic faulting process. We use the same source model to compute low- and high-frequency ground motions separately. After incorporating the nonlinear site effect into high-frequency synthetics, we combine the low- and high-frequency predictions to generate broadband ground motions.

To model kinematic faulting process, we divide the fault of the mainshock into subevents. For each subevent we prescribe the slip history. In our kinematic model each subevent represents a point source with parameters consisting of the local slip amplitude, secant (average between hypocenter and a point on the fault) rupture velocity (Day, 1982), and rise time—all of which are poorly constrained for future earthquakes. In order to allow for our inadequate *a priori* knowledge we describe these parameters as random variables with probability distribution functions that are bound by estimates of the parameters based on past earthquakes.

The stochastic distribution of a source parameter (slip amplitude, risetime, or rupture velocity) is constructed by filtering a white noise using a k^{-2} decay filter in the two-dimensional wavenumber domain. The filter has the form (Mai and Beroza, 2002):

The stochastic distribution of a source parameter (slip amplitude, risetime, or rupture velocity) is constructed by filtering a white noise using a k^{-2} decay filter in the two-dimensional wavenumber domain. The filter has the form (Mai and Beroza, 2002):

$$F(k_x,k_y) = \left[1 + (k_x C_L)^2 + (k_y C_W)^2\right]^{-1}, \tag{1}$$

where C_L and C_W are coherence lengths along strike and dip, respectively. They are calculated using the empirical relations obtained by Mai and Beroza (2002):

$$\log_{10}(C_L) = -2.5 + M_w/2, \text{ and } \log_{10}(C_W) = -1.5 + M_w/3. \tag{2}$$

The white noise for slip amplitudes is generated by the truncated Cauchy probability distribution (Lavallée and Archuleta, 2003):

$$p(D) = C\frac{1}{1 + [(D - D_0)/\kappa)]^2}, \qquad 0 \le D \le D_{\max}, \tag{3}$$

with the constraint: the maximum slip of the target event $D_{\max}= 3.5\overline{D}$; C is the normalizing factor. The factor κ is determined in such way that the generated random variables have a mean value of $\overline{D}$. We adjust D_0 to match the energy radiated from our kinematic source model with the target radiated energy. Although several studies have been done to estimate the radiated energy directly from recorded ground motions (e.g. Choy and Boatwright, 1995; Boatwright *et al.*, 2002; Venkataraman *et al.*, 2002), we simply use Brune's ω^{-2} source spectrum (Brune, 1970) to calculate the target energy radiated from a large event. Given the rupture velocity, risetime, and slip-rate function defined below, we find that $D_0 \approx 0.5\overline{D}$.

Dynamic modeling of complex rupture process (e.g. Oglesby and Day, 2002; Guatteri, et al. 2003) shows that the areas of large slip correlate with fast rupture velocity. However we use the

secant, not the local, rupture velocity. We assume that the correlation between secant rupture velocity and slip is about 30%. The finite fault inversions indicate that most earthquakes in California have an average rupture velocity around 0.8Vs. We calculate the secant rupture velocities V_r using a uniform distribution between 0.6 and 1.0 Vs. The rupture velocities generated from this distribution have a mean value of 0.8Vs.

Normally large slip requires long durations. Otherwise peak value of slip velocity could be very large. So we set the correlation between rise-time and slip to 60%. For the rise time we consider a Beta distribution:

$$p(\tau) = C\left(\tau - \tau_{\min}\right)\left(\tau_{\max} - \tau\right)^2; \quad \tau_{\min} \le \tau \le \tau_{\max} \tag{4}$$

We assume $\tau_{\max} = 5\tau_{\min}$ where $\tau_{\max}$ is determined by matching the spectral levels at high frequency, basically infinity, in Brune's ω^{-2} model.

The choice of the functional form of slip rate for a point source (used for each sub-element on the fault) is a principal component in the prediction of broadband ground motion. We construct a slip rate function as

$$\dot{s}(t) = \begin{cases} C_N[0.7 - 0.7\cos(\pi t/\tau_1) + 0.6\sin(0.5\pi t/\tau_1)] & 0 \le \tau < \tau_1 \\ C_N[1.0 - 0.7\cos(\pi t/\tau_1) + 0.3\cos(\pi(t-\tau_1)/\tau_2)] & \tau_1 \le \tau < 2\tau_1 \\ C_N[0.3 + 0.3\cos(\pi(t-\tau_1)/\tau_2)] & 2\tau_1 \le \tau < \tau \end{cases}, \tag{5a}$$

where

$$C_N = \pi/(1.4\pi\tau_1 + 1.2\tau_1 + 0.3\pi\tau_2), \tag{5b}$$

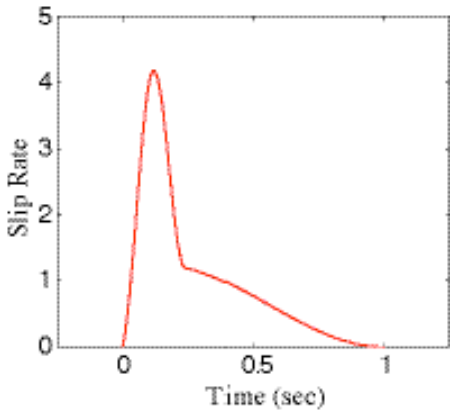

Figure 1. Slip Rate Function

and τ is risetime, $\tau_1 = 0.12\tau$, $\tau_2 = \tau - \tau_1$. Both the first and second derivative of this slip rate function has a non-zero value at starting time. This feature implies that the initial phase of the simulated rupture process will radiate high-frequency energy. Also note (Figure 1) that the slip rate function is not symmetric—characteristic of slip rate functions determined in dynamic simulations (e.g., Day, 1982; Andrews, 1976).

Having the kinematic source model, we use a three-dimensional (3D) Earth model to calculate synthetic ground motions for frequencies up to one to two Hertz. The 3D model incorporates the geometry of the geology in the area, including the deep basin structures. It is expected that the 3D synthetics will maintain the proper phasing and amplitude of surface waves. However, we cannot extend such calculations to high frequency (>2 Hz) because we have poor knowledge of the subsurface geological medium on a scale of tens to hundreds meters. (And we have insufficient computational facilities even at the present stage of the high-performance computing.) We use a layered Earth models (1D) and a FK code (Zhu and Rivera, 2001) to generate ground motions up to high frequencies (e.g. 20 Hz). The 1D computations are very efficient for obtaining high-frequency synthetics, but they cannot account for the scattering effects that reduce the influence of radiation pattern on high-frequency ground motions and increase the duration of the ground motion. This disadvantage can be partly overcome in our 1D computations by randomly perturbing the given strike, dip, and rake angle

of faulting. Let φ representing strike, dip, or rake angle of a point source on the fault plane, we express the φ as a frequency-dependent random value (Pitarka, *et al.*, 2000; Zeng and Anderson, 2000):

$$\varphi_i = \begin{cases} \varphi_0 & f \le f_1 \\ \varphi_0 + (f - f_1)/f_2 - f_1)((2r_i - 1)\varphi_p, & f_1 < f < f_2 \\ \varphi_0 + (2 * r_i - 1) * \varphi_p & f_2 \le f \end{cases}, \quad (6)$$

Where φ_0 is the given value of strike, dip, or rake angle of a fault; φ_p is maximum perturbation can adding on φ_0; r_i is a random number uniformly distributed between 0 and 1; the subscript i denotes the index of point source. The perturbation on φ_0 linearly increases when the frequency f varies from f_1 to f_2. In this study we use f_1=1 Hz and f_2=3Hz.

We use a 1D nonlinear approach (e.g., Bonilla *et al.*, 1998; Hartzell *et al.*, 2004) to compute the soil nonlinear response near surface. To do so, we need first to deconvolve the synthetics to get the up-going wave at the bedrock level. The 3D synthetics could contain a strong signal due to surface waves, which are difficult to deconvolve to bedrock level. Therefore we calculate the nonlinear response using only 1D synthetics as input. After incorporating the nonlinear site effects, the high-frequency components of 1D ground motions and 3D synthetics are stitched together to form a broadband time histories of ground motions.

Validation of the Method

The method is evaluated using the data set from the 1994, Mw 6.7, Northridge earthquake. This earthquake is a good event because of the complex geology of the Los Angeles area. In our prediction, we chose the fault model based on Hartzell *et al.* (1996). Fault strikes 122° and dips 40° to the southwest. The fault plane extends from a depth 5 to 21 km, with a fault downdip width of 20 km. The hypocenter is at 34.211°N, 118.546°W and a depth of 17.5 km.

To obtain kinematic modeling of source process of Northridge earthquake, the fault area is first discretized into 128 rectangular elements along strike and 128 elements down dip for a total of 16384 subfaults (or point sources). The spatial distribution of slip, secant rupture velocity, and rise time are then generated using the method described in last section. During this procedure a 1D velocity model is adopted to calculate the seismic moment and rupture velocity of each point source. The corner frequency of Northridge earthquake is specified at 0.14 Hz—one over the effective time that is defined as the shortest dimension of fault (20 km) divided by an average rupture velocity (2.8km/s). We also scale the seismic moments of point sources such that their summation equals the total moment of $1.14*10^{19}$ Nm. Rake has an average angle of 105°.

We calculate synthetic ground motions at 30 stations selected by the SCEC implementation interface management. The records of the Northridge earthquake and site classifications of these stations are provided by Graves (leader of the SCEC validation project). We use Version 3 of the SCEC 3D seismic velocity model (Magistrale *et al.*, 2000) and our 3D finite difference method to calculate the synthetic ground motions for frequencies up to one Hertz. In this calculation, we set the lowest shear wave velocity to be 550m/s, requiring a minimum grid interval of 100m. For attenuation we prescribe Q_S

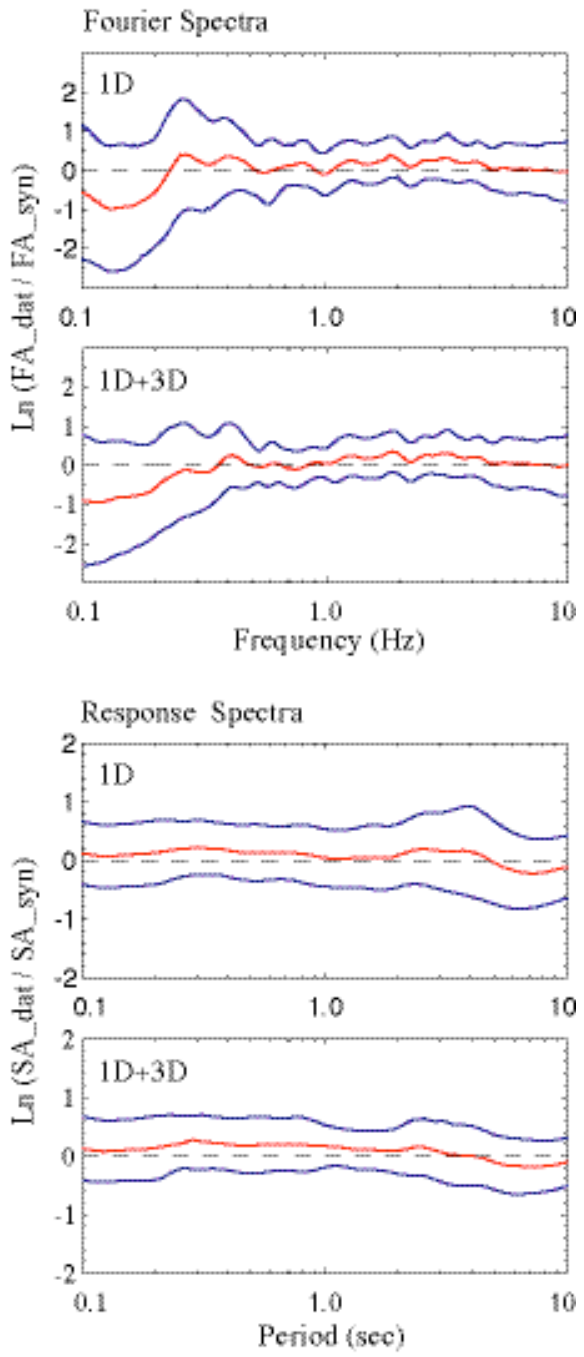

Figure 2. Average bias with standard error for our broadband simulations using 30 stations. Top is Fourier amplitude and bottom is response spectrum. 1D refers to results from a purely 1D model; 1D+3D are for low frequencies in 3D and high frequencies in 1D.

$$Q_S = \begin{cases} 0.06V_S & V_S \le 1000 \\ 0.12V_s, & 1000 < V_S < 2000 \\ 0.16V_S & 2000 \le V_S \end{cases} \quad (7)$$

with Q_P =1.5 Q_S, where shear wave velocity V_S has the units of m/s. This same Q structure is used for the 1D models. We use two layered Earth models (1D): one for rock site, another for soil site. We generate ground motions up to 10 Hz with the FK code of Zhu and Rivera (2001). In the 1D calculation we divide each subfault into a 3x3 finer grid and sum the Green's functions at the nine grid points with a rupture time delayed to obtain the Green's functions for the subfault.

We use NOAHW program (Bonilla *et al.*, 1998; Hartzell *et al.*, 2004) to compute the soil nonlinear response near surface. The stress-strain relation in NOAHW is specified in this study according to modulus reduction curves of EPRI (1993). Silva et al. (1998) developed shear wave velocity profiles for NEHRP site categories B, BC, C, D, and E. We have adopted these velocity profiles in this study. We also average the velocity profiles of categories C and D for computing the nonlinear site response at stations classified as CD. Only the 1D synthetic ground motions at surface are linearly deconvolved to the bedrock with depth of 300 m.

Combining low-frequencies components of 3D synthetics and high-frequencies component of 1D results, we get broadband synthetic ground motions. At present, we choose a crossover frequency at 1 Hz. With better 3D structure and with our improved FD code, we can efficiently simulate low-frequency wave propagation in a 3D structure up to 2Hz. The comparison of the broadband predictions and ground motions records is made by calculating the bias and the standard error of predicted ground motion parameters, such as peak ground accelerations (PGA), peak ground velocity (PGV), Fourier amplitude spectra, or response spectra. Following the work of Abrahamson *et al.* (1990) and Schneider *et al.* (1993), the bias of predictions is given by

$$B = \frac{1}{N}\sum_{i=1}^{N}[\ln(O_i) - \ln(S_i)] \tag{8a}$$

and the standard error is estimated by

$$E = \sqrt{\frac{1}{N}\sum_{i=1}^{N}[(\ln(O_i) - \ln(S_i)) - B]^2} \tag{8b}$$

where N is the number of all the horizontal components of records, S_i and O_i are synthetic and observed ground motion parameter, respectively. Figure 2 plots the bias and standard error versus the frequencies (or period) for acceleration Fourier spectra and 5% damped response spectra. The average bias of Fourier spectra over 30 stations and both horizontal components are close to zero from the frequency 0.3 to 10 Hz. The large negative values of bias below 0.3 Hz, which indicates over-prediction, are mostly because the data are high-pass filtered. The predicted response spectra have no significant bias over period range 0.1 to 10 second. Note that the response spectra has no large bias this feature does not mean the prediction fit the data well in long period, just because ground motion accelerations have very small amplitudes among long period. The standard errors are about 0.5 (natural logarithm), similar to the results of other SCEC researcher. The synthetics obtained by combining 1D and 3D have a slightly smaller the misfit at low frequencies.

Discussion and Conclusions

The method presented in this study is for predicting broadband ground motion time histories from a future scenario earthquake. It uses the spatial distributions of randomized source parameters to describe the kinematic source process. We have validated the method using data from the Northridge earthquake. Our model bias and standard error is similar to the best results obtained from other techniques. In our validation, however, the faulting model used to generate the broadband synthetics is not constrained by an a priori inversion result; and an average velocity profiles for each site category is used for computing nonlinear response.

The variation of ground motions predicted by our method results from both modeling and parametric uncertainties in our prediction. The standard error estimated from validation can be used as the measurement of the modeling uncertainty. The parametric uncertainty consists of the uncertainties in our input parameters: 1) seismic moment, corner frequency of the mainshock, geometry of the main fault (strike, dip, length, and width), and location of the hypocenter. Effects of the uncertainties in these parameters can be considered by performing several predictions separately using a wide range of values for these parameters. Moreover, as we compute a wide range of ground motions for a particular target event, we can also determine whether a specific event, such as Northridge, falls within the computed range.

References

Abrahamson, N., P. Somerville, and C. Cornell (1990). Uncertainty in numerical strong motion predictions, in *Proc. Of the Fourth U.S. National Conference on Earthquake Engineering*, Vol. 1, 407-416.

Andrews, D. (1976). Rupture propagation with finite stress in antiplane strain, *J. Geophys. Res.* **81**, 3575-3582.

Boatwright, J., L. Choy and L. Seekins (2002). Regional Estimates of radiated seismic energy, *Bull. Seism. Soc. Am.*, **92**, 1241-1255.

Bonilla, L., D. Lavallée, and R. Archuleta (1998). Nonlinear site response: Laboratory modeling as a constraint for modeling accelerograms, in *Proc. The Effects of Surface Geology on Seismic Motion,* Yokohama, Japan, **2**, 793-800.

Brune, J.N. (1970). Tectonic stress and the spectra of seismic shear waves from earthquakes, *J. Geophys. Res.*, **76**, 5002.

Choy, L. and J. Boatwright (1995). Global patterns of radiated seismic energy and apparent stress, *J. Geophys. Res.* **100**, 18,205-18,228.

Day, S.M. (1982). Three-dimensional simulation of spontaneous rupture: the effect of nonuniform prestress, *Bull. Seism. Soc. Am.*, **72**, 1881-1902.

EERI (Electric Power Research Institute) (1993). Guidelines for determine design basis ground motions, *Electric Power Research Institute Technique Report EPRI TR-102293*

Field, E. H., H. A. Seligson, N. Gupta, V. Gupta, T. H. Jordan, and K. W. Campbell, Loss estimates for a Puente Hills blind-thrust earthquake in Los Angeles, California, *Earthquake Spectra*, **21**, 329-338.

Guatteri, M., P. Mai, G. Beroza, and J. Boatwright (2003). Strong ground-motion prediction from stochastic-dynamic source models, *Bull. Seism. Soc. Am.*, **93**, 301-313.

Hartzell, S., P-C Liu, and C. Mendoza (1996). The 1994 Northridge, California, earthquake: Investigation of rupture velocity, rise time and high-frequency radiation, *J. Geophys. Res.*, **101**, 20091-20108.

Hartzell, S., L. F. Bonilla, and R. A. Williams (2004) Prediction of nonlinear soil effects, *Bull. Seism. Soc. Am.*, **94**, 1609-1629.

Kramer, S. (1996). *Geotechnical Earthquake Engineering*, Prentice-Hall, Inc., Upper Saddle River, New Jersey.

Lavallée, D. and R. Archuleta (2003). Stochastic modeling of slip spatial complexities for the 1979 Imperial Valley, California, earthquake, *Geophys. Res. Lett.*, **30**, 1245, doi:10.1029/2002GL015839.

Magistrale, H., S. Day, R.W. Clayton, and R. Graves (2000). The SCEC southern California reference three-dimensional seismic velocity model Version 2, *Bull. Seism. Soc. Am.*, **90**, S65-S76.

Mai, P.M., and G.C. Beroza (2002). A spatial random field model to characterize complexity in earthquake slip, *J. Geophys. Res.* **107**, 1-21.

Oglesby, D. D. and S. M. Day (2002) Stochastic faulting stress; Implications for fault dynamics and ground motion, *Bull. Seism. Soc. Am.* **92**, 3006-3021.

Pitarka, A., P. Somerville, Y. Fukushima, T. Uetake, and K. Irikura (200). Simulation of near-fault ground-motion using hybrid Green's functions, *Bull. Seism. Soc. Am.*, **90**, 566-586.

Silva, W., R. Darragh, and N. Gregor (1998). Reassessment of site coefficients and near-fault factors for building code provisions, *Pacific Engineering and Analysis Report 98-HQ-GR-1010.*

Schneider, J., W. Silva, and C. Stark (1993). Ground motion model for the 1989 M 6.9 Loma Prieta earthquake including effects of source, path, and site, *Earthquake Spectra*, **9**, 251-287.

Shaw, J., A. Plesch, J. Dolan, T. Pratt, and P. Fiore (2002). Puente Hills blind-thrust system, Los Angeles, California, *Bull. Seism. Soc. Am.*, **92**, 2946-2960.

Venkataraman, A., L. Rivera, and H. Kanamori (2002). Radiated energy from the 16 October 1999 Hector Mine earthquake: Regional and teleseismic estimates, *Bull. Seism. Soc. Am.*, **92**, 1256-1265.

Zeng, Y. and J. Anderson (2000). Earthquake source and near-field directivity modeling of several large earthquake, EERI Proceedings for the Sixth International Conference on Seismic Zonation.

Zhu, L. and L. Rivera (2001). Computation of dynamic and static displacement from a point source in multi-layered media, *Geophys. J Int.*, **148**, 619-627.